

Molecular Weight and Molecular Weight Distributions in Synthetic Polymers

Thomas Carl Ward

Department of Chemistry and Polymer Materials and Interfaces Lab, Virginia Polytechnic Institute and State University, Blacksburg, VA 24061

Polymers distinguish themselves from other species by the presence of a repeating unit or units within a molecular chain. The production of synthetic polymeric materials always involves creation of molecules having varying numbers of these repeating units for both kinetic and thermodynamic reasons. Of those key parameters shown in Table 1 which determine how a polymer will perform in the solid, in solution, or in the melt, molecular weight distribution (MWD) is usually the dominating factor, often influencing the other parameters. The details of semicrystalline polymer morphologies is a good example of MWD playing a role in another parameter. The existence of this distribution of molecular weights has fascinated polymer scientists since the beginning of the quantitative aspects of the discipline in the second quarter of this century. It is hard to overstate the importance of polymer MWD both from an industrial and an academic point of view. To emphasize this point, a few examples will be cited.

Much theoretical attention has been directed toward finding the role of MWD in the rheology of polymer solutions and melts (1). Models of the flow behavior of polymer liquid systems rely heavily on accurate MWD data in order that the predictions of such treatments might be evaluated adequately. On the other hand, on the practical side, it is observed that performance-oriented criteria such as environmental stress crack resistance and permeability to gases also heavily depend on MWD (2). The scientific literature is filled with examples of both theoretical and applied MWD studies (e.g., see 3, 4). The methods of production (e.g., catalyst type), of processing procedure (e.g., milling, foaming, casting, extruding) and the subsequent environmental exposure (e.g., moisture, radiation) all enter into the shaping of a polymer's MWD. Hence a wide range of scientific groups usually has a keen interest in the subject. It is fair to ask a question concerning the exposure of these persons to such an important area. In the traditional undergraduate curriculum, unfortunately, there is little or no exposure to MWD's. Yet, it should be clear that the ability to describe mathematically, to characterize experimentally, and to correlate physical properties with MWD must be high on any list of skills required in polymer science and engineering.

In this introductory treatment an attempt is made to provide sufficient educational material on MWD's for students interested in polymers without engaging in extensive derivations. Attention is drawn to several of the more prominent models for predicting MWD in a pedagogical way. In addition, the current most popular instrumental methods which might be applied to characterize MWD are reviewed with an emphasis on the physical chemistry of each. The reader interested in more detailed discussions of hardware or in rigor of the theoretical development will find two excellent recent reviews (5, 6). Textbooks in polymer science may be helpful in providing alternative fundamental discussion (7, 8, 9).

The Description of Molecular Weight Averages and Molecular Weight Distribution

Two curves shown in Figure 1, and to be discussed below, illustrate a typical way of presenting MWD data. The ordinate is generally the weight fraction of polymer chains having a certain number of repeating units, denoted here by i , the de-

Table 1. The Polymer Parameters

| | |
|----------------------------------|--|
| 1. Chemical Composition | Is the polymer a homopolymer or a combination of more than one repeating unit? What is the architecture of chain assembly? |
| 2. Molecular Weight Distribution | What are the proportions of chains having different numbers of repeating units in a sample? |
| 3. Stereochemistry | Do cis/trans isomers exist? Can there be stereoisomers (tacticity), and what is their distribution along the chains? |
| 4. Topology | Are the chains linear, branched or crosslinked? |
| 5. Morphology. | What are the details of the structure of the solid polymer? |
| 6. Miscellaneous | Additives, surface features may be present. |

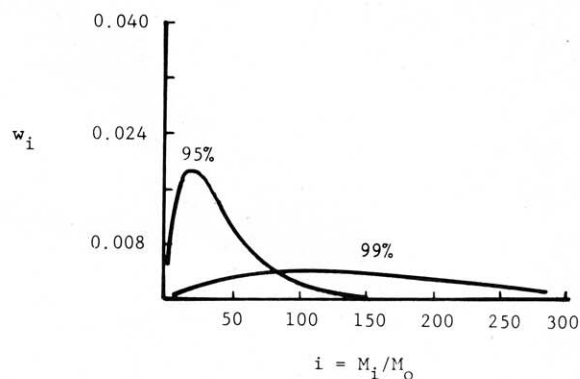


Figure 1. Two molecular weight distributions for random step growth polymerizations having different conversions, p , shown in percents.

gree of polymerization. The notation DP is also in common use for degree of polymerization. The abscissa shows the number of these repeating units per chain. If we ignore the chain ends, which are usually chemically different from the repeating units, the DP scale is related to that for molecular weight through the relationship $M_i = iM_0$, where M_0 is the molecular weight of a repeating unit. Although two smooth curves are drawn in Figure 1, polymer DP's and molecular weights must be discrete measures. We find that for visualization purposes and to aid in analytical manipulation of the MWD data the continuous functions which are sketched prove most convenient. The smooth curves also suggest that the ordinate be interpreted as the probability density for finding molecular weights (MW) between MW and $(MW + dMW)$.

Also, it is apparent that it might be appropriate occasionally to plot the mole fraction, n_i , of polymer having i repeating units as the dependent variable, rather than the weight fraction. This comment will be amplified in the paragraphs which follow. In either discrete or continuous presentations of MWD data the areas under the curves should be equal to unity.

While the curves in Figure 1 have actually been drawn from a theory, one would like to establish such information experimentally. An operation of this kind is termed fractionation. In the ideal case we would like to pick apart a sample's MWD in order to identify both the number of molecules of each size and their absolute molecular weight. MWD plots could then be constructed. This concept is illustrated schematically in Figure 2 where the weight fraction of polymer having molec-

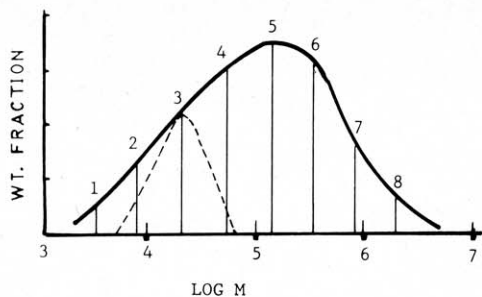


Figure 2. Hypothetical MWD indicating sharp fractions, and a broad fraction, 3.

ular weight M_i is plotted as a function of $\log M_i$ in recognition that for very broad distributions a linear MW scale would be inadequate. The vertical, numbered lines in Figure 2 would represent some of the results of this hypothetical fractionation process, the length of each line giving the weight fraction of each species. A histogram would result from continuing the experiment. The lines would be so tightly placed on the $\log M_i$ scale that the smooth curve in Figure 2 would appear.

What is found in real fractionation experiments (discussed below) is that it is only possible experimentally to separate somewhat narrower distributions from the whole polymer by fractionation, as illustrated by the dashed line at position 3 in Figure 2. Nevertheless, in order to clarify the concept of average molecular weights, it can be imagined that the results of a "perfect fractionation" were obtained as displayed in Table 2 for a few of the lower molecular weight members of a sample. If each DP is again denoted by i , while N_i and $W_i = N_i M_i$ are the number of molecules and the mass in the i th class of polymer, respectively, then their sums over all classes give the total number of molecules and total mass of polymer. Then the number and mass fractions are evaluated easily. This suggests that two valuable averaging procedures be defined for the distribution, emphasizing different portions of the spectrum of molecular sizes. The first of these is called the number average molecular weight (\bar{M}_n) and is formed by simply summing the product of the mole fraction of each species and its molecular weight. The second average is referred to as a weight average molecular weight (\bar{M}_w); in this case one sums the weight fraction of each species times its molecular weight to find the average.

The mathematical formulation of the two average molecular weights is:

$$\bar{M}_n = \frac{\sum_{i=0}^{\infty} N_i M_i}{\sum_{i=0}^{\infty} N_i} = \sum P_{n,i} M_i \quad (1)$$

$$\bar{M}_w = \frac{\sum_{i=0}^{\infty} W_i M_i}{\sum_{i=0}^{\infty} W_i} = \sum P_{w,i} M_i = \frac{\sum N_i M_i^2}{\sum N_i M_i} \quad (2)$$

where $\rho_{n,i}$ and $\rho_{w,i}$ may be interpreted as the probabilities of randomly selecting molecules of type "i" on a number or on a mass basis, respectively, from a sample. This latter identification correctly suggests that mathematical manipulations of eqns. (1) and (2) might conveniently be made using probability generating functions (10) although this will not be pursued in this article.

The number average molecular weight calculation is seen to be equivalent to taking the total weight of a sample of macromolecules and dividing that by the total number of molecules which were contained therein, usually in moles. Hence, any colligative property measurement can provide, in principle, an \bar{M}_n although not with equal sensitivity. Colligative properties are known to depend on the total number of solute particles, regardless of size, which are present in a dilute solution. Adopting a more statistical position, we notice that \bar{M}_n is also the ratio of the first moment to the zero moment of the distribution, both moments taken about zero.

By contrast, the weight average molecular weight is seen to depend not only on *how many* molecules of each type are present, but also on the *mass* of that species. Equation (2)

Table 2. The Hypothetical Fractionation of a Polymer

| "size" | i | N_i , molecules | $M_i \times 10^{20}$, g/molecule | W_i , g |
|------------|-----|-------------------|-----------------------------------|-----------|
| ○○○ | 1 | 3 | 300 | 900 |
| ○○○○○ | 2 | 2 | 600 | 1200 |
| ○○○○○○○ | 3 | 1 | 900 | 900 |
| ○○○○○○○○○○ | 4 | 2 | 1200 | 2400 |
| ● | ● | ● | ● | ● |
| ● | ● | ● | ● | ● |
| ● | ● | ● | ● | ● |

Table 3. Relative Contributions of Different Molecular Weights to the Average Values

| N_i , moles | $M_i/10^3$, g/mole | $N_i M_i/10^3$ | $N_i M_i^3/10^3$ |
|---------------|---------------------|-----------------|-------------------|
| 10 | 10 | 10^2 | 10^4 |
| 100 | 100 | 10^4 | 10^8 |
| 100 | 400 | 4×10^4 | 6.4×10^9 |
| 10 | 1000 | 10^4 | 10^{10} |

indicates that for a MWD the weight average is calculated by finding the ratio of the second moment about zero to the first moment about zero. The two definitions are related through the equality $\bar{M}_n \bar{M}_w = \sum P_{n,i} M_i^2$. Experimentally, the \bar{M}_w may be calculated from light scattering results on dilute polymer solutions. As will be presented below, the intensity of scattered radiation is found to be proportional to the DP in addition to the total number of dissolved molecules, thus biasing the measurement of average molecular weight toward larger species. Other avenues to \bar{M}_w will be briefly presented in later discussion.

Ratios of higher moments of the distribution are also important in describing certain polymer properties. In the same sense as above, when the third moment is divided by the second moment, eqn. (3), the Z-average molecular weight is the result.

$$\bar{M}_z = \frac{\sum_{i=0}^{\infty} N_i M_i^3}{\sum_{i=0}^{\infty} N_i M_i^2} \quad (3)$$

An even heavier influence is placed on the high molecular weight "tail" of the MWD by this average. The viscosities of molten polymers at low rates of deformation are found to be quite sensitive to \bar{M}_z .

A simple *gedanken* experiment will conclude this introduction to the MWD and its averages. If we imagine that molecules are selected at random from an MWD and then replaced, a sampling process occurs. Further, suppose that as molecules are selected they are classified according to their molecular weights, M_i . If, after a large population has been selected, an average is taken for MW, the result would be \bar{M}_n . The second part of this experiment is a repeat of the first, except that now the *repeating units* are selected at random. Obviously, molecules with more repeating units would be selected more often. In fact, the probability of a molecule being selected would be proportional to its degree of polymerization rather than being a random event. At the conclusion of this second experiment, large molecules would have been prejudicially sampled from the population. An average now made across the data yields a weight average molecular weight.

In order to see the disproportionately large contribution of large molecules toward average molecular weights involving the higher moments of the distribution, a simple example has been provided in Table 3. Four types of molecules were selected from a hypothetical polymer sample; with N_i and M_i for each being listed. Terms in the numerators of the definitions for \bar{M}_n and \bar{M}_z are compared in the last two columns. All molecular weights are observed to contribute significantly to

Table 4. Survey of Polydispersity

| Definition | Polymerization Process | Ratio Range |
|--|------------------------|-------------|
| $\frac{\bar{M}_w}{\bar{M}_n} \geq 1.0$ | anionic | 1.02 |
| | step growth | 1.5- 2.0 |
| | radical | 2.0- 5.0 |
| | coordination olefin | 5 -25 |
| | random branching | large |

the calculation in the case of \bar{M}_n , while the lighter molecules may be neglected in the sum leading to \bar{M}_z . We note, in addition, that only 10 molecules of one million g/mole contribute more to the third moment sum than 100 molecules of 400,000 molecular weight units. The point here is that the presence of a very small number of very large molecules can have an enormous influence on any physical or chemical property of a polymer which is a function of the higher moments of the molecular weight distribution.

A quick comparison of the breadth of any MWD is obtained by taking the ratio of weight average molecular weight to number average molecular weight and is called the polydispersity of the system. In Table 4 this ratio is tabulated for a number of common polymerization classes. In the unobtainable case where all macromolecules of a sample had the same number of repeating units, a lower limiting value of 1.00 would be achieved for the polydispersity. Depending on polymerization conditions, reaction mechanism, and subsequent polymer environmental history, breadths of MWD's are seen to be quite different. The first three systems listed in Table 4 may be modeled mathematically from reasonable assumptions; the resulting MWD's are discussed in the following section.

The Variety of Molecular Weight Distributions

In this section we will examine three common MWD's. Each can be derived from the principles underlying the appropriate polymerization mechanism. These MWD's will be characterized in terms of two independent variables. The *DP*, or *i*, is one variable; the second is a parameter which indicates the degree of advancement of the reaction process in converting monomer to polymer. This latter parameter may be couched either in kinetic or in stoichiometric terms we will define. Stoichiometrically, the fractional degree of conversion, $0 \leq p \leq 1$, will indicate progress of the reaction. On the other hand, a kinetic chain length arising from the three elementary reactions of initiation, propagation, and termination sometimes is interpreted to provide conversion information. The most convenient representation for these MWD's uses the probabilistic forms $P_{n,i}$ and $P_{w,i}$ of eqns. (1) and (2) so that

$$\bar{M}_n = M_0 \sum_{i=0}^{\infty} i \cdot P_{n,i} \tag{4}$$

$$\bar{M}_w = M_0 \sum_{i=0}^{\infty} i \cdot P_{w,i} \tag{5}$$

Often it is more convenient to manipulate a continuous distribution rather than the discrete distributions just discussed. A major reason for preferring the switch is the ease of doing certain integrations as opposed to the analogous sums. Generalizing eqns. (4) and (5) in this fashion yields

$$\bar{M}_n = M_0 \int_0^{\infty} i \cdot P_n(i) di \tag{6}$$

$$\bar{M}_w = M_0 \int_0^{\infty} i \cdot P_w(i) di \tag{7}$$

where $P_n(i)$ and $P_w(i)$ are continuous probability densities on a number and weight basis, respectively. The curves in Figure 1, when fitted by an analytical function, would be examples of $P_w(i)$ plotted versus *i*.

A popular continuous function for MWD's is the Schultz distribution as shown below:

$$P_n(i) = \frac{b^a i^{a-1} e^{-bi}}{\Gamma(a)} \tag{8}$$

where *a* and *b* are constants and $\Gamma(a)$ is the gamma function of the parameter *a*. Using the definitions of number and weight average molecular weight in eqns. (6) and (7), we find that on integrating and using the properties of the gamma function

$$\bar{M}_n = M_0 a/b \tag{9}$$

$$\bar{M}_w = M_0 (a + 1)/b \tag{10}$$

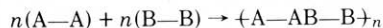
The two experimental molecular weight averages are thus sufficient to determine the entire distribution. Extension of this treatment to \bar{M}_z is left as an exercise.

Specific examples of the use of these descriptive concepts will now be generated.

The Random Distribution

Step polymerization reactions may be modeled by assuming that the probability of addition of each repeating unit to a growing linear chain is a totally random event, all molecular weights competing equally. All sizes of chains also grow simultaneously; the weight fraction of monomer rapidly approaches zero. This is found to be in excellent agreement with the facts, provided diffusional effects (such as are found in rigid, rod-like polymers) are not operative. The condensation of adipic acid with hexamethylene diamine to form nylon 6,6 is one good example of the model.

Schematically this random polymerization could be shown as



if we understand that the functionalities A and B may react only with each other to produce the chemical linkage AB. Starting with equal concentrations of the two functional groups, *n*, the fractional conversion *p* is seen to be equal to the probability that a randomly selected A or B group has reacted. Thus for an *i*-mer

$$P_{n,i} = p^{i-1} (1 - p) \tag{11}$$

since (1 - *p*) is the probability of finding an unreacted (hence terminal) unit in the reaction mixture. Multiplying $P_{n,i}$ by *i* to bias the MWD for chain length, as described above, and renormalizing the distribution

$$P_{w,i} = \frac{i \cdot P_{n,i}}{\sum i \cdot P_{n,i}} = i p^{i-1} (1 - p)^2 \tag{12}$$

Figure 1 actually was produced by plotting eqn. 12 for *p* = 0.95, and then 0.99, and subsequently connecting the points. The average molecular weights for a random distribution follow easily from eqns. (4) and (5).

$$\bar{M}_n = \frac{M_0}{1 - p} \tag{13}$$

$$\bar{M}_w = M_0 \frac{(1 + p)}{(1 - p)} \tag{14}$$

The stringent requirements for exact stoichiometry, monomer purity, and for an absence of side reactions became apparent if the random distribution is to hold. Suppose we substitute *p* = 0.999 in eqn. (13). If M_0 were 100 g/mole, this 99.9% conversion is seen to be necessary in order to get \bar{M}_n to equal 100,000 g/mole. On the other hand, \bar{M}_w would have reached 199,900 g/mole at this point. Both *MW*'s are very respectable figures for commercial polymers of this class. For this random distribution the polydispersity is given by $1 + p$, closely approaching 2.0, as the cited example demonstrates for even relatively low *MW* polymers.

The Poisson Distribution

In certain ionic polymerizations which occur without termination or transfer of the growing ion to another species, and where all chains begin to grow essentially simultaneously, a unique molecular weight distribution arises. If the initiation of polymerization is very rapid compared to the propagation, and highly pure systems are maintained, all of the monomer is consumed by the active molecules. The situation is quite different from a random polymerization in that the ionic species compete for monomer, and not for each other, in order

to react. Use of a sodium naphthalene initiator will cause styrene to polymerize anionically in this fashion. All molecular weights produced in the reaction are of about the same value and actually follow a Poisson distribution.

Kinetic arguments which invoke a constant concentration of active ionic groups and a bimolecular elementary reaction scheme can be used to derive the Poisson distribution (7, 9). The analysis introduces a new quantity called the kinetic chain length, ν , which is a measure of the degree of conversion of monomer to polymer, analogous to p in the random distribution discussed above. Changing as the reaction proceeds, at any instant in the polymerization the kinetic chain length is calculated easily from the equation

$$\nu = \frac{[M(0)] - [M]}{[C^*]} - 1 = \bar{i}_n - 1 \approx \bar{i}_n \quad (15)$$

where the monomer concentration, $[M]$, is initially $[M(0)]$, and $[C^*]$ is the concentration of chains initiated. The factor of unity is insignificant in most cases. Thus, the kinetic chain length closely approaches the number average degree of polymerization, \bar{i}_n . Since the fully reacted chains are still active ions, addition of more monomer to the system increases the average molecular weight, provided impurities which might force the chains to terminate are excluded. The suitably descriptive phrase "living polymerization" expresses the ability of these chains to grow, given more monomer. If a second monomer type susceptible to an anionic mechanism were sequentially added to a living polymer, a block copolymer would result.

The actual kinetic equations for ionic polymerization will not be given. However, on integration they yield the following Poisson probabilities based on numbers of molecules or on weights of molecules

$$P_{n,i} = \frac{e^{-\nu} \nu^{i-1}}{(i-1)!} \quad (16)$$

$$P_{w,i} = \frac{ie^{-\nu} \nu^{i-1}}{(i-1)!(\nu+1)} \quad (17)$$

This is an extremely narrow MWD. For a kinetic chain length of just 50, small for this type of polymer, the probability $P_{w,i}$ of a chain being produced with $i = 50$ is 0.0552 compared to values of 0.0329 for $i = 59$ and 0.0173 for $i = 41$, respectively. Insertion of eqn. (17) into eqn. (2) leads to

$$\bar{M}_w = M_0 \left(\frac{\bar{M}_n^2 + \bar{M}_n - 1}{\bar{M}_n} \right) \quad (18)$$

Using $\bar{M}_n = M_0(\nu + 1)$, and eqn. (15), the polydispersity ratio for the Poisson MWD is found to be

$$\frac{\bar{M}_w}{\bar{M}_n} = 1 + \frac{\bar{i}_n - 1}{\bar{i}_n^2} \approx 1 + \frac{1}{\bar{i}_n} \quad (19)$$

which reinforces the observation that a very narrow distribution is obtained. At even modest molecular weight averages, the commercial anionic polymerization of styrene results in polymer where the monodisperse limit is approached. Typically, values of polydispersity of about 1.02 or less can be achieved.

Free Radical Polymerization MWD

As in ionic polymerizations, when free radical mechanisms are involved in polymer production, kinetic arguments are convenient for deriving MWD's and the appropriate averages. Reactivity is again assumed to be independent of molecular weight. The kinetic chain length is also the choice for the variable representing the degree of conversion of monomer to polymer. Kinetically, ν is now interpreted as the ratio of the rate of chain propagation to chain termination. In other words, if we require a steady state of radicals, ν describes how much monomer is consumed per death (or birth) of an active chain. In the simple example presented here, the only termination considered will be by disproportionation. This means that two free radicals deactivate each other without the chains combining. In this case $\nu = \bar{i}_n$. (If the chains combined on termination $\nu = 2\bar{i}_n$.) Other types of radical termination mecha-

nisms are possible but will be ignored in this treatment. The rate equations indicate that ν is inversely proportional to the square of radical initiator concentration and directly proportional to monomer concentration. Thus ν is a function of reaction time and changes as the conversion of monomer to polymer advances. We will assume that the overall conversion is low (<10%) so ν is approximately independent of time. More detailed analyses not making this presumption will be expected to predict a broader MWD than the one found below.

When the rates of initiation and termination of free radicals are equal (steady state) it can be shown that within the framework of our model

$$P_{n,i} = \frac{1}{\nu(1+1/\nu)^i} \quad (20)$$

$$P_{w,i} = \frac{i}{\nu^2(1+1/\nu)^i} \quad (21)$$

The average values of molecular weight follow, exactly as in the treatments of random and Poisson MWD's, by forming the sums in eqns. (4) and (5):

$$\bar{M}_n \approx M_0 \nu \quad (22)$$

$$\bar{M}_w \approx 2M_0 \nu \quad (23)$$

More exact equations are available for any degree of conversion (see e.g., reference 11). Within the approximations of the model, a polydispersity approaching 2 is expected, just as for the random distribution. In fact, an alternative derivation of the free radical MWD described in this section is based on eqn. (11) where p is now taken as the instantaneous probability of a propagation step out of the set of propagation and termination reactions

$$p = \frac{\text{Rate Propagation}}{\text{Rate Propagation} + \text{Rate Termination}} \quad (24)$$

The random distribution formulas may be used as before on insertion of eqn. (24) with little error in the final results.

The Characterization of Molecular Weight and Molecular Weight Distribution

The literature reveals that many methods have been developed for the determination of molecular weight and MWD. No attempt has been made to be comprehensive in the following survey. The focus, rather, has been on current, widely-used experiments. It is convenient to divide these approaches into ones which provide only average values of molecular weight as opposed to those which attempt to identify the full MWD functions. Further subdivisions may be made into absolute and relative categories as determined by the need or absence of a standardization step in the experiment. These lists are found as Tables 5 and 6.

All of the MWD characterizations covered in this article require converting the liquid or solid polymer into a dilute solution and maintaining that solution throughout the experiment. Occasionally this may require high temperatures and corrosive solvents, as is the case with poly(ethylene terephthalate). In ebulliometry (boiling point change) and vapor phase osmometry the sensitivity of the experiment is affected also by the choice of solvent. Solubility of polymers is a stronger function of kinetic and diffusion effects than is found to be true in low MW compounds. Concerns about solubility are not trivial in polymer characterization problems. It should be mentioned as well that the ubiquitous presence of fillers, plasticizers, antioxidants, and other additives in commercial polymer samples has to be considered intelligently before any of the methods of Tables 5 and 6 are attempted.

Table 5 lists some absolute methods for obtaining average molecular weight. It can be seen that different experiments provide different average values as well as dramatically contrasting effective ranges. Several of the characterizations may have to be used in a complementary fashion in order to span all the molecular weights of interest in a laboratory, e.g., oligomers on the one hand to polyolefins which run into the millions of g/mole on the other.

Table 5. Absolute Methods of Molecular Weight Measurement

| Method | Obtained | Range, g/mole | Sample Size | Comment |
|------------------|------------------------------------|----------------|-------------|-------------------------------|
| end group detm. | \bar{M}_n | up to 25,000 | moderate | how many active ends? |
| osmometry | \bar{M}_n | 15,000–750,000 | moderate | automated, reasonable |
| ebullimetry | \bar{M}_n | up to 100,000 | small | fast, low sensitivity |
| light scattering | \bar{M}_w | 2000– 10^7 | moderate | conformation information also |
| ultracentrifuge | $\bar{M}_z, \bar{M}_w, \text{MWD}$ | 2000– 10^7 | small | costly, time consuming |

Table 6. Relative Methods of Molecular Weight Measurement

| Method | Obtain- ed | Range, g/mole | Sample Size | Comment |
|--------------------------|---------------|-----------------------|----------------|---|
| solution viscosity | \bar{M}_v | 15,000– 10^6 | small | economical |
| vapor phase osmometry | \bar{M}_n | up to 25,000 | small | moderate cost and time |
| size exclusion | MWD | up to 5×10^6 | small | fast, automated, high temp., calibration? |

Also in Table 5 some comments regarding the minimum quantity of sample and other pertinent features of the method have been provided and will be expanded below. A useful rule-of-thumb is that several grams or less are usually necessary in all examples. Additional special requirements are frequently found to be important in choosing one method over another as shown in the table.

Of the absolute techniques listed, only osmometry, end-group determinations, and light scattering are explored below in more detail. All are in wide use in the polymer community at this time. Ebullimetry, in practice, requires considerable experimental skill, generally on non-commercial apparatus, and provides low precision. A recent review chapter cites the merits and disadvantages of ebullimetry (12). Cryoscopy (observing freezing point changes) was not listed above but offers features similar to ebullimetry (11). The ultracentrifuge is a powerful analytical instrument capable of giving information on MWD as well as $\bar{M}_z, \bar{M}_w, \bar{M}_n$. Prior applications have been in large part directed to biological materials, typified by proteins. However, this situation is changing as the demand for MWD data has grown with the recognition of its importance. Several types of ultracentrifuge experiments exist; they differ substantially in the total time required for completion and in the specific information which is gathered. However, the procedure in all circumstances is unusually lengthy when compared to other approaches presented in Table 5. Because of the relative rarity of the ultracentrifugation method for studying synthetic polymers, no additional elaboration will be presented. However, excellent introductory material may be recommended (7, 13).

In Table 6 relative methods for finding average molecular weights and MWD's are shown. In each of these, the raw data obtained are later modified by a calibration procedure in order to make absolute MW assignments. As was true for absolute methods, a variety of ranges of molecular weight are susceptible to analysis depending on the technique.

The following material on relative MW methods concentrates first on the solution viscosity determination of average molecular weight because of the prevalence of this method and its favorable economics. A viscosity average molecular weight, \bar{M}_v , is obtained from such a determination and its definition will be provided below. Size exclusion chromatography (SEC) is also featured in the discussion. It provides direct information on the MWD rather than on an average of some type. Furthermore, it lends itself to automation and is quite rapid. Primarily for these reasons there has been an explosion of interest in SEC in the last ten years.

End-Group Determination

When a situation arises where a polymer has terminal groups which differ in some fashion from the repeating structure itself, it may be possible to chemically or spectro-

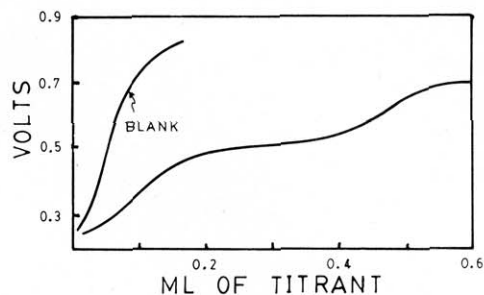


Figure 3. Potentiometric titration of bisphenol-A based polysulfone oligomers with tetraethylammonium hydroxide.

scopically determine the concentration of these unique functionalities in a solution of the polymer. Implicit in any approach to use end groups to "count" chains present in the solution is a clear-cut relationship defining the (moles of active chain ends/moles of chains) ratio, f . Given this knowledge, an average molecular weight is evaluated straightforwardly as $(c \times f) \div m = \bar{M}_n$, where c is the grams of polymer sample per cc of solution, and m is the measured number of moles of active chain ends per cc of solution.

Linear step-reaction polymers frequently fall in the favorable category of having unambiguous numbers of active terminal functions (see the random distribution above). An example of a step growth end-group measurement is illustrated in Figure 3. The unknown sample studied was a poly-(arylene ether) sulfone oligomer terminated by phenolic units. This material was later incorporated into block copolymers (14, 15). The chemistry of preparation insured that there would be exactly two of these ends per chain. Since the phenol is somewhat acidic it could be potentiometrically titrated by a base, tetra-alkyl ammonium hydroxide in this instance. Simple inexpensive equipment was found to provide accurate \bar{M}_n 's of oligomers of up to 26,000 g/mole. The same cited references also discuss a sensitive ultraviolet spectroscopic technique for measuring a similar end group in some polycarbonate oligomers. Any attempts to titrate with strong base as above rapidly cleaved the polycarbonate backbone, providing impetus for development of the alternative spectroscopic analysis. This point with respect to the potential degradative or complicating side reactions should be kept firmly in mind when wet chemical titrations are undertaken to find MW's.

It is worthwhile pointing to some of the troubles associated with end-group analysis. The presence of branching, or of uncertain stoichiometries in step-reaction polymerizations also suggest that end-group methods be applied with caution; ambiguities in f may be large in both instances. Where two possible terminal functionalities are produced from a polymerization, e.g. acid or alcohol in polyesterification, both concentrations will usually need to be calculated to find \bar{M}_n . Only special circumstances allow end-group determination to find \bar{M}_n of the products accurately of free radical polymerizations; this is partially the result of the high molecular weights usually encountered, but also it is due to uncertainties about the nature of the terminals. Obviously, as the size of the macromolecules increases the percentage of chain ends decreases. An upper limit is reached rather quickly on the molecular weights which are susceptible to end-group analysis. In general, this is approximately 25–30,000 g/mole; although, given certain especially responsive terminal functionalities,

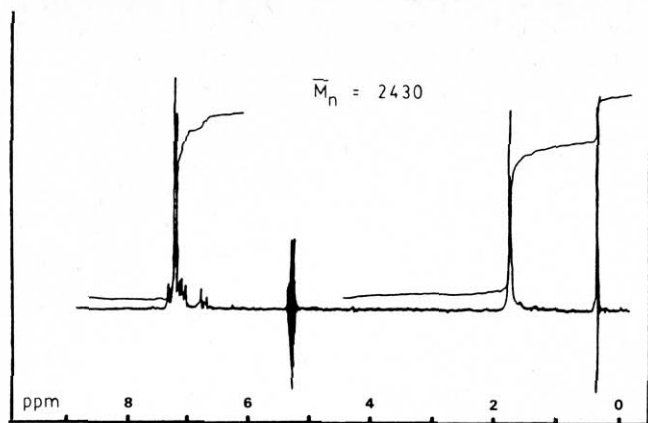


Figure 4. Proton NMR of trimethylsilyl ether terminated bisphenol-A polycarbonate oligomer. The silicon methyl proton to aromatic proton ratio was used to calculate \bar{M}_n .

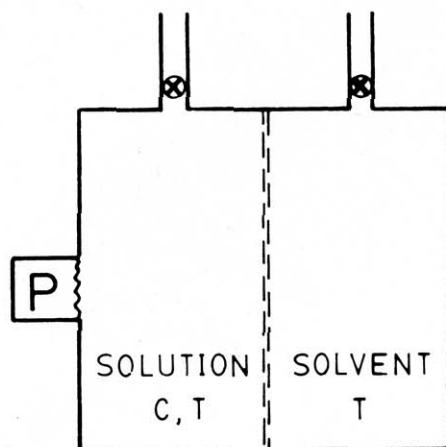


Figure 5. Schematic of osmometer showing pressure transducer, P , and solution of concentration C , and temperature, T .

higher molecular weight observations might be possible.

Occasionally, the sensitivity problem limiting end-group analysis can be circumvented by making derivatives of the chain ends. The accuracy of end-group methods obviously improves as more sensitive types of spectroscopy are focused on the problem; derivatives can offer a route to alternative instruments. One might anticipate that a UV chromophore found at, or derivatized on, an end group would provide sensitive spectroscopic opportunities. Radioactive or fluorescent tags would be even better. A final example illustrating derivitization is found in Figure 4 and involves the use of NMR spectroscopy (16). The material being investigated was a polycarbonate derived from bisphenol-A which had been capped on the ends with a trimethylsilyl ether. By observing the peak intensity ratio of methyl protons on methyls bonded to silicon to the aromatic protons of the bisphenol-A, it was possible to get a very good estimate of \bar{M}_n .

Osmometry

Osmometry has proven to be a convenient way to measure number average molecular weight for many years. This colligative property is based on the fact that certain semi-permeable membranes may be constructed which are transparent with respect to penetration by solvent molecules but which prevent the transport of macromolecules. The Gibbs free energy of the solvent is known to be lowered by the presence of solute. Pure solvent thus passes through the membrane in order to lower the free energy of the system. Hence, if a thermostated cell is constructed, as shown in Figure 5, and pure solvent is placed on one side of the membrane while solvent plus polymer is located on the other side, a pressure gradient will develop. This process will continue until an equilibrium is reached in which the free energy change due to the pressure

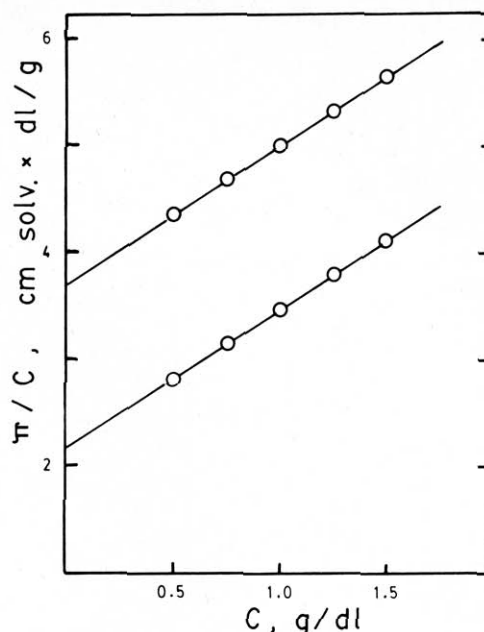


Figure 6. Typical osmometry data treatment for two samples having different molecular weights but equal second virial coefficients in solution.

rise just equals the free energy change due to dilution of the solution. The equilibrium pressure developed is called the osmotic pressure, usually denoted by the symbol π .

Elementary thermodynamics may be applied to the osmotic equilibrium to show that (17)

$$\frac{\pi}{c} = RT \left(\frac{1}{\bar{M}_n} + A_2c + A_3c^2 + \dots \right) \quad (25)$$

where c is the concentration of solution in g/cc and R and T have the usual meanings. Dilute solutions and a constant temperature were assumed in this derivation. We note that eqn. (25) is a power series in the concentration. In order to obtain \bar{M}_n an extrapolation procedure yielding π/c at the limit of infinite dilution is required. As c approaches zero all intermolecular interactions vanish and the theory becomes exact. Eqn. (25) indicates that a graphical treatment of osmometry data produces lines having zero concentration intercepts inversely proportional to \bar{M}_n . Often a $(\pi/c)^{1/2}$ versus c plot is more nearly linear and provides exactly the same extrapolated point.

Results of some idealized membrane osmometry experiments are given in Figure 6 for two polymers dissolved in a "good" solvent. Two molecular weight averages of the same polymer were investigated as is apparent from the intercepts. What sort of information might be extracted from the observation that the lines in Figure 6 appear to be parallel? Equation (24) reveals that A_2 , known as the second virial coefficient, is the slope of these lines, since c is quite small. It can be shown that A_2 is related to the strength of the interactions between solvent and polymer in dilute solution. The larger the value of A_2 , and hence the slope of a π/c versus c osmometry plot, the stronger the interactions. As the solvent power or the temperature of the solution is varied, A_2 will also change. Because of the flexibility of dissolved polymers they may assume many different solution conformations. In better solvents, polymer-segment/solvent contacts lower the energy of the system causing the chains to expand their conformation. The opposite behavior can be anticipated when "poor" solvents are used. In the special case where A_2 becomes zero the osmometry plots are horizontal. The chains will be in a coiled conformation. This "theta condition" will be discussed in the viscosity section of this article.

Judicious membrane selection is crucial in osmometry experimentation. The available membranes actually contain a distribution of pore sizes. Hence, the largest pores set the

useful permeability limit. Should an MWD contain molecules having sizes that overlap the permeability limit, erroneous conclusions will be drawn. Even in a polymer of $\bar{M}_n = 25,000$ g/mole there may be significant amounts of materials with $MW < 15,000$ g/mole, leading to large errors if the lower permeability limit in the selected membrane was 15,000 g/mole. A simple calculation will show that 0.1% (wt.) of impurity having $MW = 100$ g/mole greatly distorts the osmotic results on a polymer having $MW = 10^5$ g/mole. (An \bar{M}_n of slightly greater than 50,000 g/mole is the result!). On the other hand, when the membrane's permeability toward smaller molecules is greatly reduced, equilibration times become inconveniently long.

Modern osmometry equipment is relatively inexpensive and rapidly evaluates \bar{M}_n . The use of strain gages and sensitive electronics to detect π has permitted cell designs where the actual volume of displaced solvent is kept to a minimum. Equilibrium times (on the order of minutes) are corresponding short. The practical range of MWD accessible to osmometers is typically 15,000 g/mole $< \bar{M}_n < 750,000$ g/mole.

Although it does not formally originate from the osmotic effect, the vapor pressure osmometry experiment has been popular for evaluating \bar{M}_n , particularly for polymers or oligomers having molecular weights of less than 15,000 g/mole. Operation of these instruments depends on the fact that a solute will lower the vapor pressure of a solvent. A device is constructed having a thermostatted chamber within which two identical temperature sensors (for example, thermister beads) are suspended in the gas above a pure solvent liquid phase. Solvent is coated on one sensor and solution on the other. Frequently, syringes are inserted into the chamber to place the drops. It follows that the presence of solution on one of these sensors and solvent on the other will finally result in a temperature differential, ΔT . We can understand the phenomenon by recognizing that the solvent vapor pressure in the solution is lower than that of the pure solvent; hence, condensation of solvent begins from the vapor filled environment. The ΔT exists due to the associated heat of condensation raising the temperature of the solution until the equilibrium vapor pressure of both drops becomes equal to that of pure solvent. A little reflection will indicate that the magnitude of this effect will depend on the solution concentration. As was established with osmometry above, the correct manipulation of the data requires extrapolation of the ΔT 's generated for several concentrations of solution to zero concentration. After a calibration of the instrument, the $(\Delta T)_{c=0}$ can be converted to \bar{M}_n of the unknown. Thus, the vapor pressure change (which is too small to measure directly) has been converted to observable temperature changes and finally to \bar{M}_n . Sensitivity of the vapor phase osmometer increases as the solute molecular weight is lowered. Particularly in the 1000–15,000 g/mole range this instrument complements the membrane osmometer nicely; it is common to find them side-by-side in modern laboratories. Solvents with higher heats of vaporization give larger ΔT values per concentration unit. Aqueous polymer solutions are therefore well suited to analysis by vapor phase osmometry.

Light Scattering

Scattered electromagnetic radiation has been used extensively for finding the weight average molecular weight of synthetic polymers (for additional information, refer to references 5, 7, 18). Information about average molecular size (conformation) is also available from the scattering data. A simplified arrangement of the components is sketched in Figure 7. The incident radiation, I_0 , is focused, and sometimes polarized and filtered (or originates from a laser in modern instrumentation), and then encounters a dilute solution of polymer from which it is scattered. In the traditional experiment the detector is able to rotate about the sample cell to record the scattered beam intensity, $I(\theta)$, as a function of the angle θ . When normalized to the total scattering volume swept

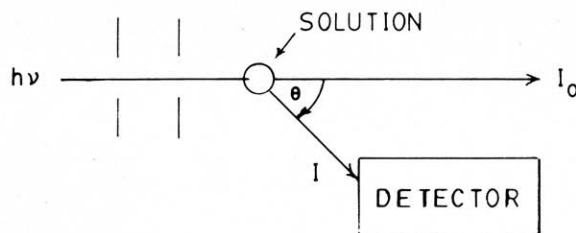


Figure 7. Schematic of essential parts of light scattering instrument.

by the beam, $I(\theta)/I(0)$ is called the Rayleigh ratio, $R(\theta)$, in honor of Lord Rayleigh's early work predicting the scattering of reemitted radiation from "small" particles. What Rayleigh discovered was that electromagnetic radiation induced an oscillating dipole in molecules which served as the source of energy dispersion according to a $(1 + \cos^2\theta)$ relationship. The $R(\theta)$ was calculated to be proportional to the square of molecular polarizability, but inversely varied as the fourth power of the incident wavelength, λ . The blue to red color variation of the Earth's atmosphere may be explained by these initial observations of Rayleigh; any size of molecules will show this scattering phenomenon. Corrections due to solvent scattering alone leads to the excess Rayleigh ratio, eqn. (26), for polymer solution characterization.

$$\bar{R}(\theta) = R(\theta) - R(\theta)_{\text{solvent}} \quad (26)$$

Modern applications of light scattering to polymers have evolved from Peter Debye's modification of the Rayleigh scattering theory above. Let's consider first the situation where the macromolecule is still smaller in average conformational dimensions than the λ of radiation by a factor of roughly 20. In this instance there is no destructive interference of a scattered wave due to interaction with radiation originating from dipoles in the same molecule. It follows from the theory that thermally induced fluctuations in both the microscopic density and the concentration may also scatter additional radiation. The majority of this new scattering has the fluctuations in polymer segment concentration as its origin. Hence, they can be translated into variations of the solution's refractive index, n , with concentration, actually appeared as $(dn/dc)^2$. A thermodynamic connection is provided by relating the osmotic pressure gradient, $d\pi/dc$, induced by the fluctuations to the free energy change that simultaneously occurs, in exactly the same fashion that lead to eqn. (25). The theory links the $\bar{R}(\theta)$ to certain fundamental constants and the osmotic virial expansion form. At this point in the discussion of "small" particle scattering, all of these quantities are connected by

$$\frac{Kc}{\bar{R}(\theta)} = \frac{1}{M} + 2A_2c + 3A_3c^2 + \dots \quad (27)$$

$$K = \frac{2\pi^2 n^2 \left(\frac{dn}{dc}\right)^2}{N_0 \lambda^4} \quad (28)$$

where N_0 is Avogadro's number. Before completing this heuristic development for larger scatterers a digression to the question "Why is the M in eqn. (27) a weight average value?" might prove fruitful in advancing our understanding of other properties that prove to be functions of \bar{M}_w .

In the derivation of eqn. (27) the amplitude of the scattered wave is found to be directly proportional to polarizability of the i th contributing molecular species, I_i . In addition, as the number of atoms in a chain increases the total molar polarizability rises proportionally. Recalling that the relationship between wave amplitude, A , and intensity, I , is always $I \approx A^2$, thus $I_i \approx M_i^2$. For any MWD, a simple extension of eqn. (2) gives

$$\bar{M}_w = \frac{\sum N_i M_i^2}{\sum N_i M_i} = \frac{\sum c_i M_i}{c} \quad (2)$$

where the second equation follows from the first on division

of numerator and denominator by the solution volume. It is reasonable that in dilute solution the total scattered intensity at some angle will be made up of the linear contributions:

$$I(\theta) = \sum N_i I_i \propto \sum c_i M_i = \bar{M}_w c \quad (29)$$

So the $R(\theta)$, which is proportional to $I(\theta)$, is easily seen to be related to molecular weight by the following,

$$\frac{c}{R(\theta)} \propto \frac{1}{\bar{M}_w} \quad (30)$$

At this point we need to account for scattering by "large" particles. Very small particles will scatter radiation symmetrically with respect to the forward and the backward directions as the $(1 + \cos^2\theta)$ dependence indicates. When the particles doing the scattering are macromolecules which exceed $1/20$ of λ in average size then there is a phase shifting of the scattered components of the incident radiation by different parts of the same molecule. This means that the angular dependence of the scattering will become different in the forward and reverse direction and also depend on polymer conformation. An angular scattering function, $P(\theta)$, enters the analysis to account for this new anisotropy of $I(\theta)$. If the polymer is assumed to have a conformation that, over time, sweeps out a spherical volume of average diameter \bar{d} , then

$$\frac{1}{P(\theta)} = 1 + \frac{16\pi^2\bar{d}^2}{3\lambda^2} \sin^2(\theta/2), \quad (31)$$

Note that this function has a limiting value of unity at $\theta = 0$.

Insertion of the angular scattering function into eqn. (27) produces the final result

$$\frac{Kc}{R(\theta)} = \frac{1}{\bar{M}_w P(\theta)} + 2A_2c + \dots \quad (32)$$

Following the pattern established in osmometry, we might expect that information on the \bar{M}_w of the dissolved polymer would be obtained through an extrapolation of $Kc/R(\theta)$ to zero concentration following experiments on several solution concentrations. Further inspection of the final equation reveals, however, that the angular function $P(\theta)$ remains as a complicating factor even as $c \rightarrow 0$. Since $P(\theta) \rightarrow 1$ as $\theta \rightarrow 0$, a double extrapolation of c and θ (referred to as a Zimm plot) produces a common intercept at $(\bar{M}_w)^{-1}$, as shown as Figure 8. The abscissa contains scaling factors k_1 and k_2 which are arbitrary and chosen to produce a reasonable grid pattern. From the slope of the $\theta = 0$ line the second virial coefficient is obtained. Average conformational information on the dissolved polymer follows from analyzing the slope of the $c = 0$ line.

Light scattering measurements traditionally have required scrupulously clean, dust-free samples in order that spurious scattering not be generated. The presence of any gel-like, semidissolved, or associated polymer causes large errors, \bar{M}_w being more sensitive to their presence than to that of smaller impurities. Copolymers with compositional distributions superimposed on the MWD require more extensive investigations in order to find \bar{M}_w . Primarily, this is a consequence of the variation of the dn/dc term with MW .

Developments in light scattering instrumentation have been rapid following the increased availability of suitable laser radiation sources. One commercially available instrument using a laser detects radiation scattered within a few degrees of the incident beam where $P(\theta)$ is essentially unity. Knowledge of dn/dc and the second virial coefficient then allows calculation of \bar{M}_w from a single Rayleigh ratio measurement. However, molecular conformational information is lost if the multiple angle study is not pursued.

Solution Viscosity

One of the oldest, and the most popular, experiments to find the average molecular weight of macromolecules derives from their ability to increase the viscosity of a solvent when they

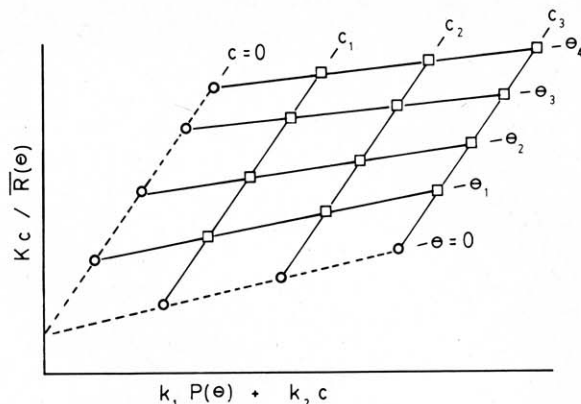


Figure 8. A Zimm-plot double extrapolation procedure. Constants k_1 and k_2 are arbitrary scaling factors. Squares are data points. Circles are extrapolated points.

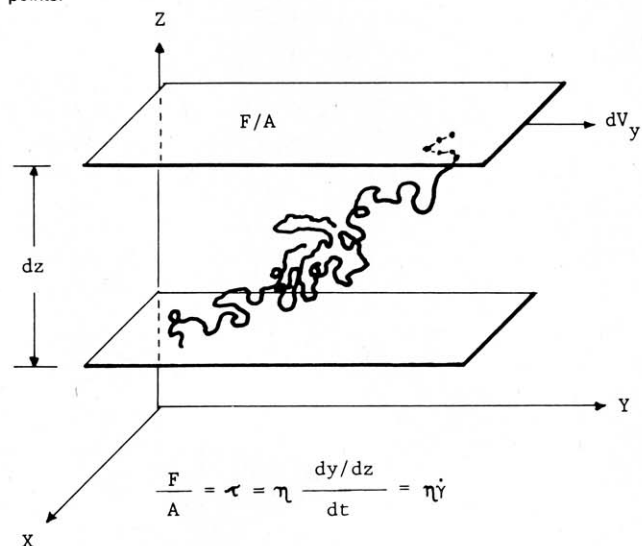


Figure 9. Newtonian viscosity of a fluid in shear between two parallel plates. F = force, A = area, V_y = velocity, τ = shear stress, $\dot{\gamma}$ = shear rate, and η = viscosity.

are placed in a dilute solution. Lying somewhere between the \bar{M}_n and \bar{M}_w , the viscosity average, \bar{M}_v , may be obtained from the magnitude of the viscosity increase plus a semi-empirical relationship having constants which must be determined by an appropriate absolute MW calibration method.

A brief review of the general viscosity concept appears in Figure 9. When momentum is transported by a fluid between two parallel planes of area A which are smoothly sheared relative to one another, a force, F , is required. Intuitively, we anticipate that more massive molecules transmit more momentum than lighter molecules, concentrations being equal. The actual hydrodynamic problem establishing this exact relationship is, however, a function of the conformation of the polymer as well as interactions between sheared polymer and solution, and quite complex. Following the second virial coefficient discussion above, we expect that it might be possible to somehow enter A_2 into a viscosity-molecular weight theory. Comments along these lines will follow later.

Newton's viscosity law describes the force required to achieve a relative velocity gradient, dV_y/dz between the plate in terms of the viscosity η as follows:

$$\tau = \frac{F}{A} = \eta \frac{dV_y}{dz} = \eta \dot{\gamma} \quad (33)$$

where τ is referred to as the shear stress and $\dot{\gamma}$ the shear rate. Instruments which keep both τ and $\dot{\gamma}$ small are best for dilute polymer solution work; macromolecules and theoretical assumptions tend to break down otherwise. It will be shown that the determination of τ and $\dot{\gamma}$ may be circumvented in \bar{M}_v calculations.

Newtonian flow is readily generated in small bore circular tubes. The essential parts of a glass capillary viscometer are illustrated in Figure 10. Many elaborations of the design exist. But, the ubiquitous nature of this instrument has derived from its low shear rates, economy, and ability to evaluate rapidly η . The essential part is the thermostated, vertically positioned capillary tube through which a known volume, V , of fluid is allowed to descend. Assuming laminar flow, and no other energy losses, the classical Poiseuille equation for tubular flow provides the functional form between the Newtonian volumetric flow rate, Q , the pressure drop, ΔP , the capillary radius and length, r and l , and the flow times, t :

$$Q = \frac{V}{t} = \frac{\pi r^4 \Delta P}{8 \eta l} \quad (34)$$

Since solvent and dilute solution have essentially the same density (and thus ΔP)

$$\frac{\eta}{\eta_0} = \eta_{rel} = \frac{t}{t_0} \quad (35)$$

where a relative viscosity has been defined by the solution to solvent viscosity ratio. We see that the experiment to find η_{rel} simply requires the careful observation of the flow times necessary for equivolume amounts of pure solvent and solution to flow through the capillary. The fractional increase in viscosity is named the specific viscosity, η_{sp} , and is useful:

$$\eta_{sp} = \frac{\eta - \eta_0}{\eta_0} \quad (36)$$

Of course, as solution concentration increases so will η —leading eventually to polymer entanglements. Only the dilute region is of interest to us for this discussion. In order to ascertain how η_{sp} is connected to MW, the solution concentration effects must be eliminated. In Figure 11 the typical dependence between the two appears showing that η is linearly varying with c . In the limit of infinite dilution a more meaningful number is obtained as we have already observed. An extrapolation of η_{sp}/c to $c = 0$ is appropriate. The intercept is called the limiting viscosity number, or intrinsic viscosity, $[\eta]$, and is formally

$$[\eta] = \left(\frac{\eta_{sp}}{c} \right)_{c=0} = \left(\frac{1}{c} \ln \frac{\eta}{\eta_0} \right)_{c=0} \quad (37)$$

Also shown in eqn. (37) is that an additional quantity, the inherent viscosity, $\ln(\eta/\eta_0)$, also extrapolates to same $[\eta]$. Four to five concentrations between 0.05 and 2 wt.% are ordinarily sufficient to identify $[\eta]$. Non-linearities which sometimes occur in the η_{sp}/c versus c line are discussed in other sources (6). As a rough estimate, when $[\eta]$ exceeds 0.50 dl/g for an unknown sample, reasonably high MW's are present.

While the intrinsic viscosity has in itself often been used to indicate in a qualitative fashion that high MW's have been achieved in a polymerization, the semi-empirical Mark-Houwink-Skurada equation

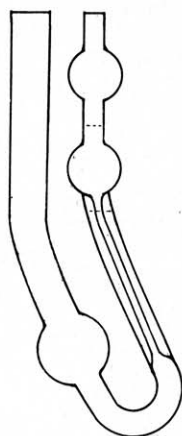


Figure 10. Essential features of a capillary viscometer.

$$[\eta] = k \bar{M}_v^a \quad (38)$$

provides the more precise connection between the two that we have been seeking. In this function k and a are constants which, in some cases, are found to apply only over certain portions of an MW range. The exponential parameter, a , varies from 0.5 for polymer/solvent/temperature combinations where the conformation of the polymer is randomly coiled, to values in the vicinity of 1.0 for thermodynamic combinations that promote extended, rod-like molecular shapes. An order-of-magnitude value for k would be 1×10^{-4} dl/g. A few of these constants are shown in Table 7 (19). As will be explained below, it is important to emphasize that for each kind of polymer both the temperature and solvent must also be specified in order to identify the two Mark-Houwink-Skurada parameters. Significant modification in the k and a values appears when there is polymer branching, especially of the long chain variety; lower $[\eta]$'s are found for branched materials than for linear topologies, MW's being equal. (This provides an avenue for estimation of long-chain branching through viscosity investigations.)

Polymer handbooks are available containing extensive tabulations of k 's and a 's (19). Obviously, in order to fit eqn. (38) it was necessary to employ one of the absolute techniques of MW measurement. In the preferred methodology, the polymer MWD is first fractionated to the extent that $M = \bar{M}_n \approx \bar{M}_w$ for each fraction, and M and $[\eta]$ evaluated. The double logarithmic plots in Figure 12 are constructed to linearize the data. Their slopes and intercepts are used to extract the two desired constants from the raw data.

In order to identify \bar{M}_v in the spectrum of MWD averages we have introduced, it is informative to consider how a whole polymer's intrinsic viscosity arises from the individual molecular contributions. The $[\eta]$ was defined for that hypothetical ideal state of zero polymer concentration. Just as in the ideal gas, all polymer-polymer intermolecular interactions vanish in this limit. Each MW class, i , independently contributes to the overall intrinsic viscosity according to the probability of its presence in the solution. Letting $[\eta]_i$ represent the intrinsic viscosity of i , and recognizing that the

Table 7. Constants for Mark-Houwink-Skurada Equation

| Polymer | Solvent | Temp. °C | a^a | $k \times 10^4$, dl/g ^a |
|---------------------------|------------|----------|-------|-------------------------------------|
| polystyrene | toluene | 25 | 0.69 | 1.7 |
| | benzene | 25 | 0.74 | 0.2 |
| poly(methyl-methacrylate) | acetone | 25 | 0.70 | 0.75 |
| | chloroform | 20 | 0.79 | 0.60 |

^a a , k may vary with molecular weight range.

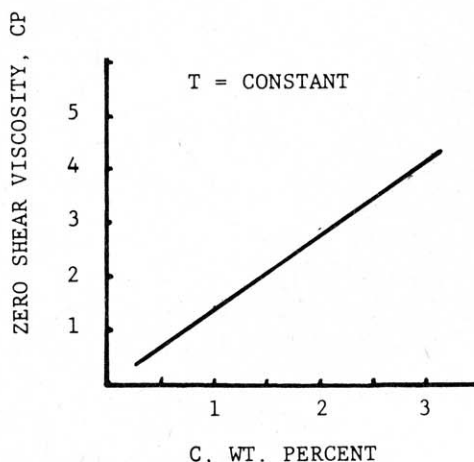


Figure 11. The typical dependence of dilute polymer solution viscosity on concentration as shear rate approaches zero.

Mark-Houwink-Skurada equation still applies to each molecular type because $\bar{M}_v = \bar{M}_n = \bar{M}_w$:

$$[\eta]_i = kM_i^a \quad (39)$$

Furthermore, the dependence on M_i in this equation makes it plausible that in assembling $[\eta]$ from its components, $[\eta]_i$, the appropriate probability for the average is $P_{w,i}$ rather than $P_{n,i}$. Substituting these ideas into eqn. (38), and assuming that k and a do not change with MW,

$$k\bar{M}_v^a = [\eta] = \sum P_{w,i}[\eta]_i = \sum P_{w,i}kM_i^a = \frac{k\sum N_iM_i^{a+1}}{\sum N_iM_i} \quad (40)$$

Solving eqn. (40) we obtain

$$\bar{M}_v = \left(\frac{\sum N_iM_i^{a+1}}{\sum N_iM_i} \right)^{1/a} \quad (41)$$

Comparing eqn. (41) to eqn. (2) leads to the observation that when $a = 1$, $\bar{M}_v = \bar{M}_w$. We note that \bar{M}_v is a function of the $(a + 1)$ th moment of the MWD divided by the first moment. Thus, it tends to be much closer to the \bar{M}_w value than it is to \bar{M}_n .

Before leaving the concept of the viscosity of dilute solutions of macromolecules, it is important to summarize one major conclusion of the early theoretical treatments (8). It was found that the $[\eta]M$ product was directly proportional to the average conformational size of a dissolved flexible polymer. Imagining a situation where solvent/polymer/temperature interactions are adjusted to the point that the polymer assumes its "unperturbed" average shape, the theory shows that

$$[\eta]M \propto (\bar{r}_0^2)^{3/2} \quad (42)$$

where we are defining a mean square end-to-end dimension of linear chains as (\bar{r}_0^2) . The special unperturbed state is referred to as the θ condition, already presented above. An infinite MW polymer would be on the verge of precipitation in this θ situation. Also, the second virial coefficient would be approaching zero as this point is being achieved. At the other extreme, better solvation of the polymer would cause an expansion of the characteristic average chain dimension as solvent-polymer contacts now lower the system's free energy. A multiplicative chain expansion factor, $\alpha \geq 1$, enters the model in order to express the average molecular size:

$$[\eta]M = \phi(\bar{r}_0^2)^{3/2}\alpha^3 \quad (43)$$

The right-hand side of eqn. (43) is referred to as the polymer hydrodynamic volume, in accordance with its dimensions, and the ϕ is a constant. Demonstrating that the Mark-Houwink-Skurada equation follows from eqn. (43) is left as a simple algebraic exercise for the reader.

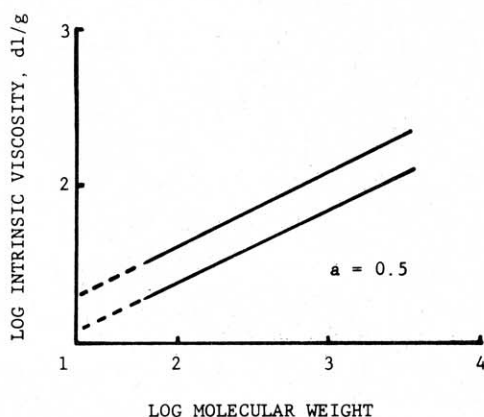


Figure 12. Determination of the Mark-Houwink-Skurada constants from data on polymer fractions. Slope of lines = a , intercept = $\log k$. The examples show $a = 0.5$, the theta condition for this polymer/solvent/temperature combination.

Fractionation

The general ideas behind fractionation have been presented in the introductory material. In practice, most of these experiments have roots in the differential in solubility which exists across a MWD. Higher MW species are less soluble, assuming constant composition if a copolymer is involved. Commonly, the solvating power, the temperature, or both may be programmed to remove selectively a portion of the MWD in a fractionation. Consequently, two basic schemes for separation exist:

- 1) *Selective solution* involves the continual improvement in the solvent power of the extractant. Lower MW's are removed first.
- 2) *Selective precipitation* requires decreasing the extractant's ability to dissolve polymer. Higher MW's are removed first.

In the literature one may find numerous elaborations on each approach. However, very narrow fractions are always the goal. For example, inert columns may be constructed which have both solvent gradients and temperature drops along their length. Polymer moving through the column continually precipitates and redissolves, leading to fractions of smaller molecules being eluted first.

A considerable amount of time and skill are required for a successful fractionation using the principles found above. For preparative scale work, however, both the major approaches are still essential to polymer science. In analytical terms they both have been supplanted largely by size exclusion chromatography which will be discussed in a separate section. Extensive documentation of introductory fractionation theory and technique is available (20, 21).

A promising recent development in separation science is called field flow fractionation (FFF). By coupling two driving forces for polymer separation, e.g., those originating from a centrifugal field applied perpendicular to a velocity gradient established in a polymer solution, impressive resolving power appears to be obtainable (22). Future development in this area will be of great interest.

Size Exclusion Chromatography (SEC)

The rapid emergence of SEC for evaluating MWD's in the 1960's has been the outstanding analytical advance in polymer characterization. Improvements in instruments and interpretations have continued up to the present; the SEC literature is extensive, not just on MWD determination, but for other applications e.g., branching evaluation, as well. Recent monographs have appeared (23). The name "gel permeation chromatography," also applied to the technique, is descriptive of the original column packing materials which were employed.

The SEC fractionation occurs during exposure of a pumped polymer solution to a distribution of micropores in a packed column. The diffusional volume accessible to smaller molecules is greater than that for the larger varieties. Consequently, larger molecules elute from the column first. Either surface-modified porous glass beads or swollen crosslinked polymer beads may be used as the microporous medium. Figure 13 contains a visualization of how a small region of a GPC sample (SAM) column packing might appear. Conceptually, we can envision the low MW polymer as traveling a much longer, more tortuous path than high MW material as it traverses the entire column. Any adsorption of polymer on the beads tends to preferentially retain large molecules, destroying resolution. Clearly, the technology thrust behind advanced GPC columns was an essential one which spurred the growth and development just noted.

Aside from the columns the SEC instrument is basically a liquid chromatograph of the HPLC variety. The essential features of modern size exclusion chromatographs are blocked-out in Figure 14. Preparation of solvent will typically consist of degassing, heating and pumping the fluid at a carefully metered, surge-free rate. Previously dissolved and

filtered polymer is placed in the moving sample stream at the point marked "inject." After fractionation in the sample column(s), one or more detectors in series are encountered which evaluate the eluting polymer concentration (mass/volume), or some other feature of the sample stream e.g., viscosity. These detectors are indicated by $\Delta 1$, $\Delta 2$, and $\Delta 3$ in Figure 14. Differential refractive index (DRI), ultraviolet absorption (UV), infrared absorption (IR), and light scattering detectors have all been exploited to advantage in SEC. A fraction collector as shown may be part of the apparatus as well. SEC is well suited for high temperature fractionations; often it is the technique of choice for polymers of limited solubility at room temperatures.

Two representative chromatograms are pictured in Figure 15. With UV, IR, or DRI detectors the ordinate of this output is proportional to the mass of polymer in the sample cell which was present at various elution volumes. Hence, we can easily normalize chromatogram peak heights to a weight fraction scale. It should be carefully noted, however, that Figure 15 will *not* be a plot of MWD until the elution volume scale is converted into an MW scale. The relative, as opposed to absolute, nature of the SEC experiment resides in this restriction.

For a number of years the appropriate calibration of SEC columns has been a significant scientific problem. In order that absolute MWD's might be obtained, narrow, well-characterized polymer fractions had to be injected into the instrument. For calibration accuracy, a matching of the standard and the unknown with respect to chemical composition and topology was necessary, solvent and column temperature being the same as well. Prior comments in this article dealing with the average conformation of dissolved macromolecules make it apparent why this was the case. For example, polystyrene and polycarbonate of identical MW would have quite different hydrodynamic volumes if dissolved in tetrahydrofuran at 50°C (as expressed quantitatively by the chain expansion factor, α). It appears that a true size separation

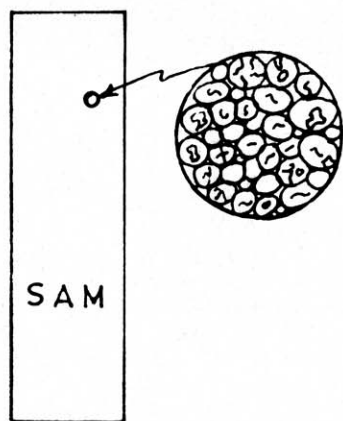


Figure 13. Expanded view of area in the packing of a size exclusion column.

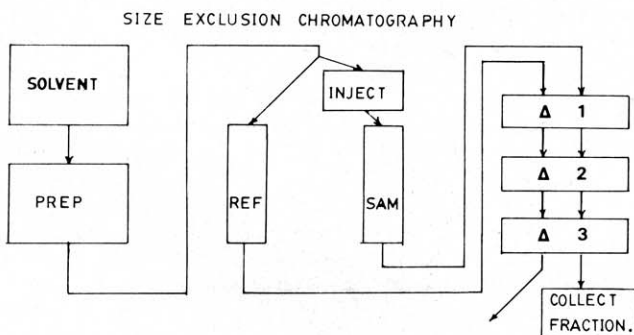


Figure 14. Essential features of a size exclusion chromatograph. The Δ 's are detectors, SAM = sample, REF = reference, PREP = pumps, degasser, etc., INJECT = sample injection port.

mechanism is operative in SEC; it is not an MW fractionation phenomenon. The calibration problem arises since matching standards are largely unavailable for new polymers, copolymers, or branched polymers. Commercial anionic (Poisson distribution) polystyrenes have been, and still are, frequently substituted as "standards" so that MW's of dissimilar polymers could be at least estimated.

A representative calibration curve is shown in Figure 16 indicating that six narrow MWD standards were injected to establish column parameters. Each standard's elution volume peak maximum was taken in conjunction with its known MW to establish the curve. The volumes shown as V_1 and V_2 bracket the column separation limits on the high and low MW ends, respectively, and result from the particular micropore size distribution in the packing. In practice, only the essentially linear portions of these plots are useful. Figure 17 illustrates the steps for obtaining the MWD for the chromatogram, given a calibration curve. The illustrated steps in Figure 17 must be followed to prevent serious distortions from entering in the MWD curve. On the order of 50 increments between V_1 and V_2 on the elution volume axis might be selected. For each of the product

$$\frac{dW}{d \log M} = \left(\frac{dW}{dV} \right) \times \left(\frac{dV}{d \log M} \right) \quad (44)$$

is calculated and plotted to give the MWD. Following similar

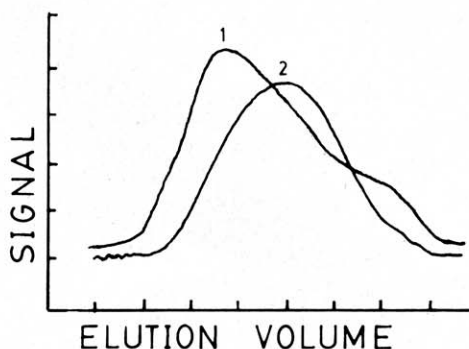


Figure 15. Chromatograms from size exclusion chromatography experiment. The signal is typically a response to polymer concentration in the flow cell. In this example, sample 1 has the higher molecular weight averages.

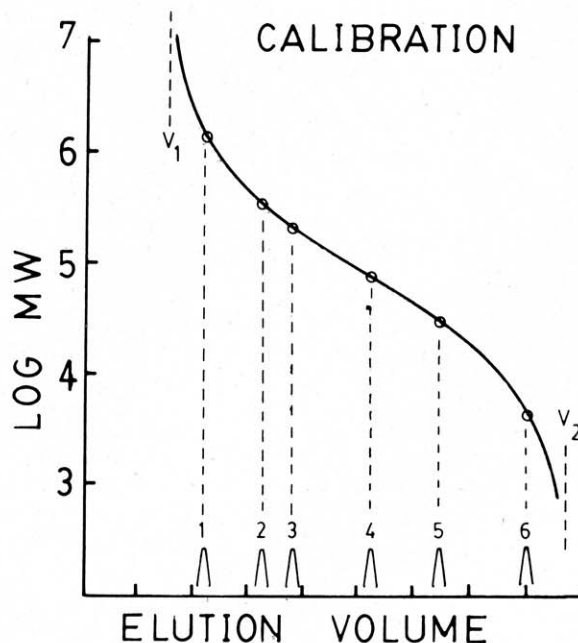


Figure 16. Calibration curve for size exclusion chromatography. Six fractions of narrow MWD were injected. Solvent and temperature must be identical with those used for unknown.

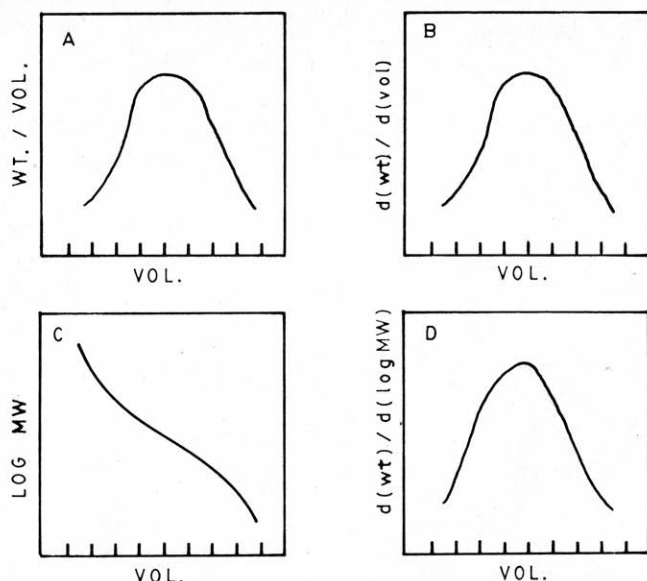


Figure 17. Steps required to convert size exclusion chromatogram to an MWD, (a) chromatogram, as in Figure 15, (b) calibration curve, as in Figure 16, inverse of the slope of this curve is calculated point-by-point, (c) normalized chromatogram, (d) the MWD is produced from a point-by-point product of (dw/dv) and $(dv/d \log M)$.

reasoning, each of these increments may be evaluated for its peak height below the chromatogram, kN_iM_i (proportional to concentration), and for M_i (from the calibration curve) so that on division of the two, kN_i is obtained. Direct substitution into eqns. (1) and (2) proves that the constant k is irrelevant for \bar{M}_n and \bar{M}_w determination. Minicomputers on modern instruments rapidly collect incremental data such as this and perform the calculations.

New aspects of SEC calibration have arisen since the recognition that the polymer's hydrodynamic volume might be the basis of an SEC fractionation (24). Indeed, this has been proven to be correct in a large number of examples. Recalling that eqn. (43) shows that the $[\eta]M$ product is the hydrodynamic volume of a dissolved polymer, a new calibration is suggested. This universal calibration is then a plot of $[\eta]M$ against elution volume, valid for all topologies and chemical compositions. Alternatively, if the Mark-Houwink-Skurada constants of the unknown, k_1 and a_1 , and of the standards, k_2 and a_2 , are known, it is easy to show that at each elution volume increment

$$\log M_1 = \left(\frac{1}{a_1 + 1} \right) \log \left(\frac{k_2}{k_1} \right) + \left(\frac{a_2 + 1}{a_1 + 1} \right) \log M_2 \quad (45)$$

relates the unknown MW to the known MW. An exceptionally careful check of the SEC universal calibration is replotted as Figure 18 (25). Excellent agreement between the poly(vinylacetate) and the polystyrene fractions was found. Highly branched materials will generally not respond to this approach, nor will polyelectrolytes. Other column calibrations are discussed in specialized references (23). Some allow broad distribution polymer to be used as the calibration standard rather than the narrow fractions.

The on-line low angle laser light scattering detector avoids the calibration problem altogether. Used in conjunction with a data processing computer, one may directly obtain the absolute MWD by SEC if there is knowledge of the specific refractive index increment, dn/dc , and if a concentration sensitive detector is also on the equipment. There are examples where, because it responds in proportion to M_w , the light scattering detector indicates the presence of trace amounts of extremely high MW material that is not detected by conventional means (26).

It is interesting to note that aqueous solutions of polyelectrolytes are also susceptible to size exclusion chromatography,

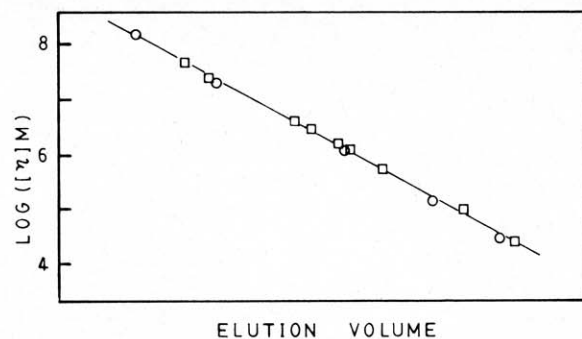


Figure 18. Evaluation of universal calibration procedure in size exclusion chromatography. \square = poly(vinyl acetate) fractions, \circ = polystyrene fractions. (Reference (25)).

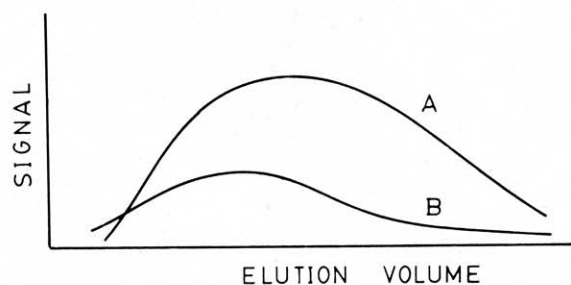


Figure 19. Comparison of size exclusion chromatographs. Original sample A has $\bar{M}_n = 15,000$ and $\bar{M}_w = 175,000$. Milled sample B has $\bar{M}_n = 35,000$ and $\bar{M}_w = 170,000$.

provided proper care is taken. Glass beads with surface modifications to prevent adsorption must be employed for aqueous phase investigations. Both polyanions (an example is poly(styrene sulfonate) (27)) and polycations (poly(2-vinyl pyridine) has been examined (28)) have been fractionated in aqueous solutions. Polyelectrolytes in solution have expanded conformations arising from the mutual repulsions of the similar charges along a chain. As might be anticipated, they consequently elute at lower SEC volumes than uncharged polymers of the same MW. Ionic strength of the solution is found to be quite important in these separations; the chains tend to be less extended as salt concentration rises, indicating that the ionic repulsions are being weakened.

In conclusion, the industrial practice of SEC often is directed toward answering the simple question of whether an MWD has been changed, irrespective of absolute values. Suppliers of polymers seeking quality control only need to look for reproducible SEC chromatograms, without worrying about the MW scale. Many processors of polymers are concerned about degradation and oxidatively or thermally induced branching occurring in the course of manufacturing. SEC is perfect for providing rapid, reliable checks for these modifications of MWD. The SEC example provided in Figure 19 is instructive of how uncalibrated chromatograms are quite useful in this regard. The SEC of material labeled A might be obtained for a virgin polymer with the specifications $\bar{M}_n = 15,000$ and $\bar{M}_w = 175,000$. Following a milling operation, the SEC would be shifted to curve B where $\bar{M}_n = 35,000$ but now $\bar{M}_w = 170,000$. Comparison of A and B without any calibration curve still clearly indicates the presence of a substantial high MW portion in A. The reversal of the sign of the change in MW on milling between \bar{M}_n and \bar{M}_w was deliberately built into this example to serve as a cautionary note. Had one selected \bar{M}_n as an index for structure-property correlations when in fact \bar{M}_w was the proper variable, serious mistakes might have resulted.

Summary

This introductory survey has indicated that MWD's play a dominant role in polymer properties, directly or indirectly.

Depending on polymerization mechanism, polymer processing, and polymer environmental exposure, MWD's are encountered that differ enormously and, in addition, may change. These two leading statements reveal that characterization of MWD through appropriate averages or, if at all possible, a full fractionation scheme is essential in polymer science. Modern instrumental methods are available which greatly facilitate the MWD measurement; these are constantly being improved, particularly with respect to automation. In the future, even further developments will probably occur in the speed and accuracy with which MWD's may be analyzed. It is likely, however, that these will be refinements based on the existing general principles described in this article.

Literature Cited

- (1) Ferry, J. D., "Viscoelastic Properties of Polymers," 3rd. Ed., John Wiley and Sons, New York.
- (2) Martin, J. R., Johnson, J. F., and Cooper, A. R., *J. Macromol. Sci.-Revs. Macromol. Chem.*, C8[1] (1972).
- (3) Agarwal, P. K., *Macromolecules*, 12, 344 (1979).
- (4) Zachasiades, A. E., Kanamoto, T., and Porter, R. S., *J. Polym. Sci., Polym. Phys. Ed.*, 575 (1980).
- (5) Slade, Jr., P. E., (Editor), "Polymer Molecular Weights," Parts I and II, V.4 of "Techniques of Polymer Evaluation," Marcel Dekker, New York, 1975.
- (6) Pollock, D. J., and Kratz, R. F., Part A, Vol. 16, "Methods of Experimental Physics," (Editors: Marton, L. and Marton, C.), Academic Press, 1980, Chapter 2.
- (7) Billmeyer, Jr., F. W., "Textbook of Polymer Science," John Wiley and Sons, New York, 1971.
- (8) Flory, P. J., "Principles of Polymer Science," Cornell University Press, Ithaca, NY, 1953.
- (9) Cowie, J. M. G., "Polymers: Chemistry and Physics of Modern Materials," Intertext Books, Aylesbury, UK, 1973.
- (10) Gordon, M., *Proc. Royal Soc.*, A268, 240 (1962).
- (11) Elias, H.-G., "Macromolecules," V.2, Plenum Press, New York, 1977.
- (12) Chapter 4 of ref. (5).
- (13) Bowen, T. J., "An Introduction to Ultracentrifugation," John Wiley and Sons, New York, 1970.
- (14) McGrath, J. E., Ward, T. C., Shchori, E., Wnuk, A. J., Viswanathan, R., Riffle, J. S., and Davidson, T. F., *Polymer Preprints*, 19[1], 109, 1978.
- (15) Shchori, E., and McGrath, J. E., *J. Appl. Polym. Sci., Appl. Polym. Symp.*, 34, 103 (1978).
- (16) Riffle, J. S., Ph.D. Dissertation, Virginia Polytechnic Institute and State University, 1981.
- (17) Moore, W. J., "Physical Chemistry," 4th Ed., Prentice-Hall, New Jersey, 1972, Chapter 20.
- (18) McIntyre, D., and Gornick, F., "Light Scattering from Dilute Polymer Solutions," Gordon and Breach, New York, 1964.
- (19) Bradrup, J., and Immergut, E. H. (Editors), "Polymer Handbook," 2nd Ed., John Wiley and Sons, 1976.
- (20) Cantow, M. J. R. (Editor), "Polymer Fractionation," Academic Press, 1967.
- (21) Tung, L. H. (Editor), "Fractionation of Synthetic Polymers," Marcel Dekker, New York, 1977.
- (22) Giddings, J. C., Myers, M. N., and Caldwell, K. D., *Polym. Preprints*, 22[1], 287 (1981).
- (23) Yau, W. W., Kirkland, J. J., and Bly, D. D., "Modern Size-Exclusion Liquid Chromatography," John Wiley and Sons, New York, 1979.
- (24) Grubisic, Z., Rempp, P., and Benoit, H., *J. Polym. Sci.*, B5, 753 (1967).
- (25) Atkinson, C. M. L., and Dietz, R., *European Polymer J.*, 15, 21 (1979).
- (26) Chromatix Company application literature, 1145 Terra Bella Ave., Mountain View, CA 94043.
- (27) Cooper, A. R., and Matzinger, D. P., *J. Appl. Polym. Sci.*, 23, 419 (1979).
- (28) Talley, C. P., and Bowman, L. M., *Analytical Chemistry*, 51, 2239 (1979).